

# Research on the Nanobainitic Features Formed in the Ultra-low Carbon Steel Non-Containing Nb and Ti Elements

Na LI <sup>a</sup>, Qingsuo Liu <sup>b\*</sup>, Haixia Zhang <sup>c</sup> and Meiju Zhao <sup>d</sup>

School of Materials Science and Engineering, Tianjin University of Technology, Tianjin 300384, China

<sup>a</sup>1061677782@qq.com, <sup>b</sup>qingsuoliu@eyou.com, <sup>c</sup>95296858@qq.com, <sup>d</sup>15222064572@163.com

**Abstract.** The XRD analysis, microstructure observation and mechanical test were used to investigate the phase composition, micromorphology and mechanical properties of the intermediate transformation products in an ultra-low carbon steel non-containing Nb and Ti elements. The results showed that even without the presence of Nb and Ti alloy compounds, the experimental steel still exhibited good Rockwell hardness level. When the steels were held for a shorter times at 450 °C, its Rockwell hardness under stayed 100s after plastic deformation at 850 °C was higher than that under cooled directly because the 100s-stayed process was benefit to the formation of nanobainite. However, when the steels were held over 30min at 450 °C, its Rockwell hardness under stayed 100s were close to that of non-stayed steel.

**Keywords:** ultra-low carbon steel; stayed process; nanobainite; Rockwell hardness

## 1 Introduction

The ultra-low carbon bainitic steel (ULCB) is highly concerned by the international engineering community in recent years [1-3]. The key possessing excellent combination of strength and toughness is to refine microstructure, especially refine bainite. Normally, cooperation of the plastic deformation at the high temperature and Nb, Ti compound precipitation was used to form sheaf-like bainite and adjust the mechanical properties of the material [4,5]. It is worth noted that the technology would be lost effectiveness, once the plastic deformation at the high temperature can't be cooperated effectively with Nb, Ti compound precipitation process.

The nanobainite has been found in the high carbon silicon-containing steel [6]. The nanobainite can put excellent mechanical properties to the steel, causing widespread concern in academic circles. From the perspective of microscopic morphology, nanobainite should be formed in ULCB by controlling the process parameters. This result is worth the wait.

---

\* Corresponding author: qingsuoliu@eyou.com

In this paper, a kind of ULCB steel non-containing Nb and Ti alloying elements is selected, and the morphological variation of the products formed by intermediate transformation under different treatment process is discussed in order to provide a theoretical support for researching nanobainite in the field of ULCB.

## 2 Experimental Procedure

The chemical composition of the experimental steel melted in the ZG-25 vacuum medium frequency induction melting furnace was Fe-0.05C-1.3Mn-0.35Ni-0.3Si-0.25Mo(wt.%). The dilatometric test was measured by Gleeble 3500 thermo-mechanical simulator. The treatment process curve of the samples was shown in Fig.1. The samples were heated to 1200°C for 5min then cooled to 850°C lower than the recrystallization temperature of the designed material and deformed plasticity amount 30%. The samples were stayed 100s or not stayed after plastic deformation at 850°C then cooled to 450°C at 15°C/s holding different times (such as indicated by p1 and p2 in Fig.1).

The transformation points of the designed material were measured by Rigaku Formastor-Digit 2 full automatic thermal dilatometer with heating at 20K/min to the high temperature for 20min then cooling down to room temperature at 40K/s. The phase composition of the samples was analyzed by Rigaku D/Max-2500V X-ray diffractometer with unfiltered  $\text{CuK}_\alpha$  radiation, at a scanning speed 8°/min, and operating at 40kV and 100mA. The Germany Carl Zeiss Axio Scope A1 microscopy was used to observe the optical microstructure of the samples. The HR-150 hardness tester was used to test the Rockwell hardness value (HRC) of the samples. The thin foils for transmission electron microscopy (TEM) were prepared by twin-jet electro polishing using an electrolyte of mixture of 5% perchloric acid and 95% methanol. The fine structures of the thin foils were observed by JEM-2100 transmission electron microscope.

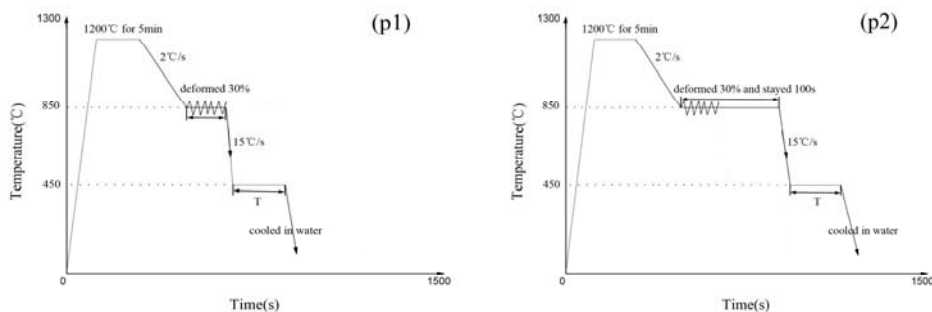


**Fig.1** Process curves of the experimental steel experienced process p1, p2

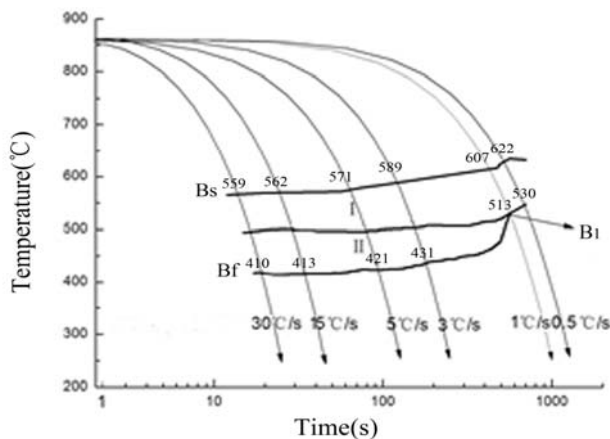
## 3 Results and Discussion

Fig.2 shows the continuous cooling transformation (CCT) diagram of the samples cooled directly to room temperature at different cooling rates after plastic deformation at 850°C. The range about 650°C-400°C in Fig.2, i.e. the intermediate transformation region was divided obviously into two parts indicated by I and II, respectively corresponding the high and low region of the intermediate transformation. The intermediate transformation start ( $B_s$ ) and finish ( $B_f$ ) temperature corresponding the samples with different cooling rates are shown in Fig.2. When the cooling rate is increased from 3°C/s to 15°C/s,  $B_s$  and  $B_f$  are

decreased from 589°C and 431°C to 562°C and 413°C, respectively.

It's worth noted that the dividing line of region I and II in Fig.2 is intersected just with  $B_f$  line under corresponding cooling rate of 1°C/s. The intersection point is denoted by  $B_f$ . It is demonstrated that the intermediate region isn't divided under cooling rate of less than 1°C/s. Bhadeshia et al. reported that nanobainite was generally formed at a lower temperature in the intermediate region for the high carbon silicon-containing steel[7]. To use it as reference, in this paper, the microstructure characteristics of the samples processed isothermally at 450°C which located just at low temperature in the intermediate region are studied.

Fig.3 shows the XRD pattern and optical micrograph of the as-cast sample annealed at 850°C. This figure represents that the microstructure of the sample consists of  $\alpha$ -phase (ferrite phase). The  $2\theta$  values of  $\alpha$ -phase diffraction peak are marked in the Fig.3(a) has the reference data for the latter analysis.



**Fig. 2** The CCT curve of the samples cooled directly after plastic deformation at 850°C

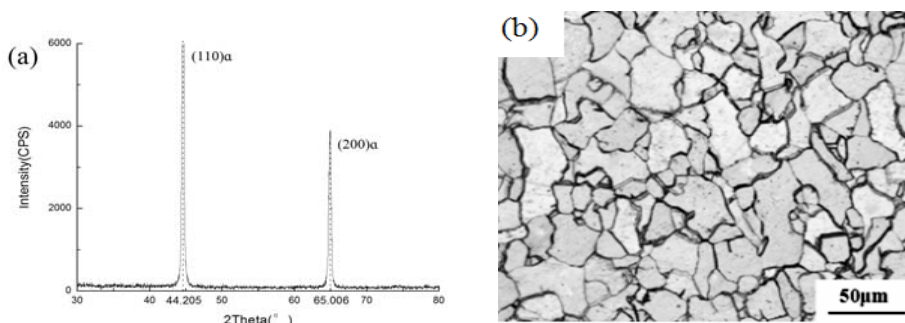


**Fig. 3** XRD pattern(a) and optical micrograph(b) of the annealed sample

The XRD patterns of the samples experienced process p1(corresponded by A) and p2 (corresponded by B) isothermal 10min at 450°C are shown in the Fig.4(a). It has been indexed that  $\alpha$  and  $\gamma$  phase contest in the samples no matter whether stayed after plastic deformation at 850°C. By compared with Fig.3(a), it is found that the  $2\theta$  coordinates of  $\alpha$  phase diffraction peak no matter  $(110)_\alpha$  or  $(200)_\alpha$  have an offset  $\Delta 2\theta$ . This represents that the microstructure feature of  $\alpha$  phase is different from that in the annealed sample. By

compared their geometrical structure, it is found that the heights of the (110) $\alpha$  and (200) $\alpha$  located in B are greater, which expresses larger numbers of  $\alpha$  phases exist in the sample experienced process p2.

Observed carefully the geometric structure of the  $\alpha$  phase diffraction peaks in Fig.4(b) of the samples experienced process p1 (corresponded by A) and p2 (corresponded by B) isothermal 30min at 450 $^{\circ}$ C, it can be found that no matter the 2 $\theta$  coordinate, geometric shape or the height are similar. This is obvious different from that in Fig.4(a). It represents that the quantity and grain size of  $\alpha$  phase in samples under isothermal longer to 30min at 450 $^{\circ}$ C are largely the same, whether or not to experience stayed after plastic deformation at 850 $^{\circ}$ C.

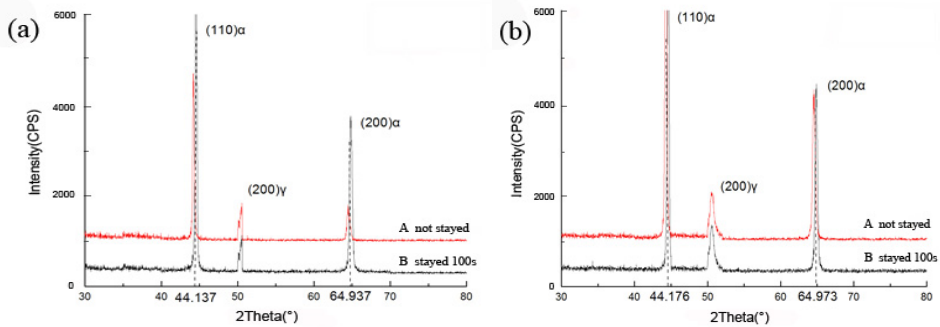


**Fig. 4** The XRD patterns of samples experienced different treatments after plastic deformation at 850 $^{\circ}$ C  
 (a) isothermal 10 min at 450 $^{\circ}$ C; (b) isothermal 30 min at 450 $^{\circ}$ C

Colligated XRD analysis results in Fig.3(a), it can be known that microstructure of the annealed sample is composed of granular ferrite. The optical micrographs of the samples isothermal 10min at 450 $^{\circ}$ C of process p1 is shown in Fig.5(a). The number of sheaf-like bainite in the field of view is significantly less than that in Fig.5(b) corresponding the samples isothermal 30min at 450 $^{\circ}$ C. The optical micrograph of the sample isothermal 10min at 450 $^{\circ}$ C of p2 process is shown in the Fig.5(c). Compared with Fig.5(a), it is found that the occupancy ratio of sheaf-like bainite in the field of view is obviously larger than that in Fig.5(a). For the same reason, the process stayed 100s after plastic deformation at 850 $^{\circ}$ C makes the dislocation tangles change into dislocation cells, which promotes the sheaf-like bainite formation. It is observed that the coarse-grain sheaf-like bainite are filled in the field of view of Fig.5(d). It is similar to that in Fig.5(b). This is consistent with the results of analyzed XRD patterns shown in Fig.4(b).

Although the staying process is not carried out after plasticity deformed at 850 $^{\circ}$ C, the continual recovery process of plastic deformation under isothermal treatment at 450 $^{\circ}$ C can't be neglected. Firstly, the dislocation tangles get weaker with increasing isothermal times. Secondly, the dislocation density in parent phase decreases gradually by means of dislocation movement and reaction among dislocations. This makes the restraining effect of dislocation tangles on bainite formation disappear gradually. Understandably, even if the stayed process after plastic deformation at 850 $^{\circ}$ C is not carried out, the micromorphology of the sheaf-like bainite formed isothermally at 450 $^{\circ}$ C for 30min is similar to that in the samples stayed 100s [8,9].

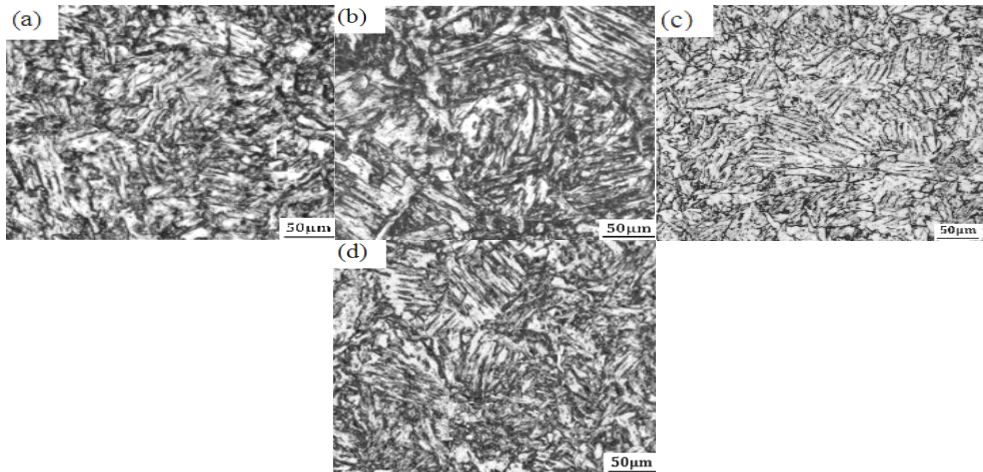


**Fig.5** Optical micrographs of the samples experienced different treatments after plastic deformation at 850°C, cooled directly to 450°C then isothermal 10min (a) and 30min (b), stayed 100s then cooled to 450°C and isothermal 10min (c) and 30min (d)

Fig.6 displays the TEM micrographs and electron diffraction pattern of the sample experienced p2. By means of the electron diffraction pattern analysis (as Fig.4b) it can be determined that the laths shown in the Fig.6(a) are bainitic ferrite. The enlarged image of diffraction spots indicated by arrow in Fig.6(b) shows that the diffraction spots corresponding to bainitic ferrite has split characteristics. It can be confirmed that the bainitic ferrite lattice have distortion characteristic. In addition, the width of bainitic ferrite lath is nanoscale corresponding with that reported by Bhadeshia [10].

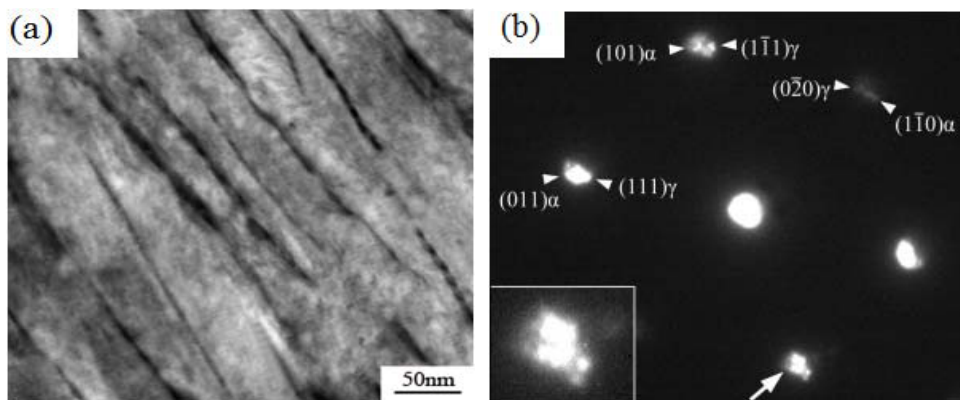


**Fig.6** The TEM micrographs(a) and electron diffraction spectrum(b) of bainitic ferrite in the sample experienced p2

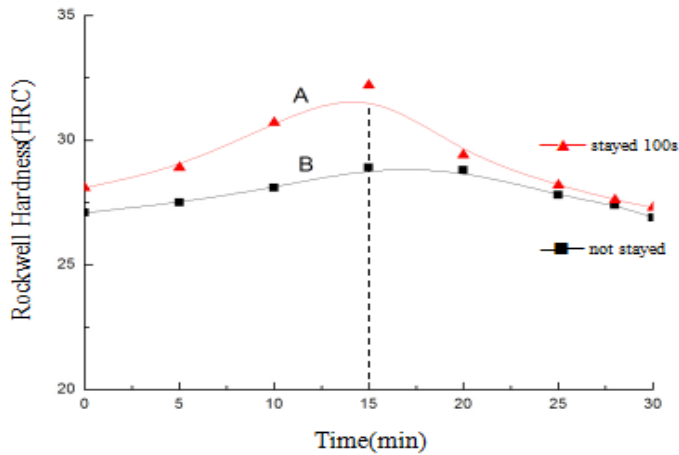


**Fig.7** The relationship curves of the HRC and Time

Fig.7 shows the relationship curves between HRC and isothermal time (T) at 450°C of the samples experienced process p1(indicated by B) and p2 (indicated by A). It's worth noted that the curvature variation of the A curve is significantly greater than that of the B curve although the curves show the approximate parabola shape.

Under p2 process, the bainitic ferrite laths with the small grains are formed naturally during short isothermal time at 450°C(such as less 15min) because of limitation of the dislocation cells, leading to high Rockwell hardness value of the sample. With extension of isothermal time the length and width of bainitic ferrite lath are increased due to the decomposition and disappearance of the dislocation cells, and then Rockwell hardness value of the sample is decreased.

For the samples experienced p1, the quantity of bainitic ferrite laths under short isothermal time at 450°C(such as less 15min) is few due to impeditive effect of the dislocation tangles on bainitic ferrite formation. Just the Rockwell hardness of the sample mainly is from the contribution of the dislocation tangles. So it is easily understood that the samples have Rockwell hardness value lower than the one of samples experienced p2. With prolonging isothermal time the dislocation tangles disappear gradually by the movement of the dislocations and reaction among dislocations, i.e. the continual recovery of deformation structure. Corresponding to this, the dislocation contribution to Rockwell hardness of the sample and the impeditive effect of the dislocation tangles on bainitic ferrite formation get weakened. The comprehensive effect of both the continual recovery of deformation structure and bainite formation makes HRC-T curve be presented parabolic shape. It is understandably that the micromorphology and Rockwell hardness level of the samples under long isothermal time at 450°C(such as 30min) should be similar whether or not stayed after plastic deformation at 850°C.

## 4 Summary

There are two intermediate transformation regions including higher and lower at CCT curve of the experimental steel. The nanobainite consisting of the approximately parallel laths with nanometer-sized width are formed in the lower intermediate transformation

region and under the conditions without Nb and Ti alloys compound. The process stayed 100s after plastic deformation at 850°C can make the nanobainite formed easily, and high hardness value of the sample be obtained in shorter isothermal time( such as less 15min ) at 450°C. For the samples not stayed after plastic deformation at 850°C, the hardness curve are flatter than that of the samples stayed 100s in isothermal condition at 450°C.

## Acknowledgement

This research was supported by Tianjin science and technology support significant project, 13ZCZDGX00800 and 15JCTPJC64600.

## References

1. J. H. Kong, C. S. Xie. Effect of molybdenum on continuous cooling bainite transformation of low-carbon microalloyed steel, *Mater Design*. 27(2006)1169-1173.
2. L. Y. Lan, C. L. Qiu, D W Zhao, et al. Microstructural characteristics and toughness of the simulated coarse grained heat affected zone of high strength low carbon bainitic steel, *Mater. Sci. Eng. A*. 529(2011)192–200.
3. C. S. Chiou, J. R. Yhng, C. Y. Huang. The effect of prior compressive deformation of austenite on toughness property in an ultra-low carbon bainitic steel, *Mater Chem Phys*. 69(2001)113-124.
4. Q. Y. Sun, Z. T. Yu, R. H. Zhu, et al. Mechanical behavior and deformation mechanisms of Ti–2.5Cu alloy reinforced by nano-scale precipitates at 293 and 77 K, *Mater. Sci. Eng. A*. 364(2004)159-165.
5. C.J. Shang, X. M. Wang, S. W. Yang, et al. Microstructure refinement of high strength low carbon bainitic steels, *Acta Metall Sin*. 39(2003)1019-1024.
6. H. K.D. H Bhadeshia. High performance bainitic steels, *Mater Sci Forum*. 500(2005)63-74.
7. H. K.D. H Bhadeshia, J. W. Christian. Bainite in steels, *Metall. Mater. Trans. A*. 21(1990)767-797.
8. A. K. De, K. D. Blauwe, S. Vandeputte, et al. Effect of dislocation density on the low temperature aging behavior of an ultra low carbon bake hardening steel, *J.Alloy.Comp*. 310(2000)405-410.
9. X. M. Wang, X. L. He, S. W. Yang, et al. Refining of intermediate transformation microstructure by relaxation processing, *Tetsu To Hagane*. 88(2002)1553-1559.
10. H.K.D. H Bhadeshia. Nanostructured Bainite, *P Roy Soc Lond A Mat* . 466 (2009) 3-18.